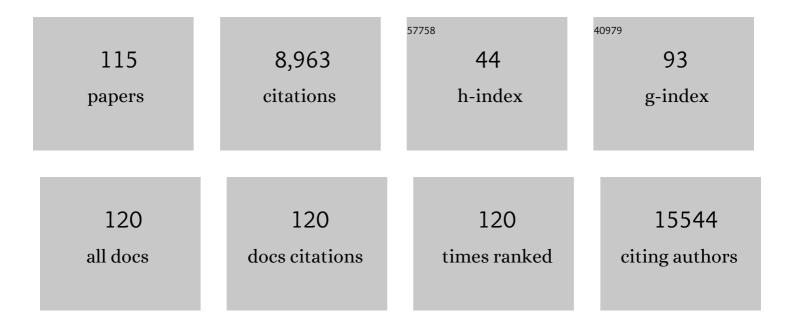
List of Publications by Year in descending order

Source: https://exaly.com/author-pdf/7757364/publications.pdf Version: 2024-02-01



#	Article	IF	CITATIONS
1	Single-Layer MoS <sub>2</sub> Phototransistors. ACS Nano, 2012, 6, 74-80.	14.6	3,103
2	ZnO cathode buffer layers for inverted polymer solar cells. Energy and Environmental Science, 2015, 8, 3442-3476.	30.8	279
3	Colorimetric Detection of Mercury Ions Based on Plasmonic Nanoparticles. Small, 2013, 9, 1467-1481.	10.0	255
4	Highâ€Performance and Tailorable Pressure Sensor Based on Ultrathin Conductive Polymer Film. Small, 2014, 10, 1466-1472.	10.0	189
5	Facile Fabrication of Highâ€Density Subâ€1â€nm Gaps from Au Nanoparticle Monolayers as Reproducible SERS Substrates. Advanced Functional Materials, 2016, 26, 8137-8145.	14.9	143
6	Optimizing the Volmer Step by Single-Layer Nickel Hydroxide Nanosheets in Hydrogen Evolution Reaction of Platinum. ACS Catalysis, 2015, 5, 3801-3806.	11.2	142
7	Enabling Light Work in Helical Self-Assembly for Dynamic Amplification of Chirality with Photoreversibility. Journal of the American Chemical Society, 2016, 138, 2219-2224.	13.7	142
8	3D Printing of Ultralight Biomimetic Hierarchical Graphene Materials with Exceptional Stiffness and Resilience. Advanced Materials, 2019, 31, e1902930.	21.0	130
9	Colloidal Synthesis and Applications of Plasmonic Metal Nanoparticles. Advanced Materials, 2016, 28, 10508-10517.	21.0	128
10	A highly active three-dimensional Z-scheme ZnO/Au/g-C3N4 photocathode for efficient photoelectrochemical water splitting. Applied Catalysis B: Environmental, 2020, 263, 118180.	20.2	126
11	A colorimetric logic gate based on free gold nanoparticles and the coordination strategy between melamine and mercury ions. Chemical Communications, 2013, 49, 4196-4198.	4.1	121
12	Platinum-nickel hydroxide nanocomposites for electrocatalytic reduction of water. Nano Energy, 2017, 31, 456-461.	16.0	119
13	Excellent electrical conductivity of the exfoliated and fluorinated hexagonal boron nitride nanosheets. Nanoscale Research Letters, 2013, 8, 49.	5.7	109
14	Scalable neutral H2O2 electrosynthesis by platinum diphosphide nanocrystals by regulating oxygen reduction reaction pathways. Nature Communications, 2020, 11, 3928.	12.8	101
15	Plasmonic Enhanced Optoelectronic Devices. Plasmonics, 2014, 9, 859-866.	3.4	100
16	Spatially Confined Assembly of Nanoparticles. Accounts of Chemical Research, 2014, 47, 3009-3017.	15.6	98
17	Phase-controlled synthesis and gas-sensing properties of zinc stannate (ZnSnO3 and Zn2SnO4) faceted solid and hollow microcrystals. CrystEngComm, 2012, 14, 2172.	2.6	89
18	Phase-controlled synthesis and photocatalytic properties of SnS, SnS2 and SnS/SnS2 heterostructure nanocrystals. Materials Research Bulletin, 2013, 48, 2325-2332.	5.2	87

#	Article	IF	CITATIONS
19	3D Anisotropic Au@Pt–Pd Hemispherical Nanostructures as Efficient Electrocatalysts for Methanol, Ethanol, and Formic Acid Oxidation Reaction. Advanced Materials, 2021, 33, e2100713.	21.0	87
20	3D Printed Mechanically Robust Graphene/CNT Electrodes for Highly Efficient Overall Water Splitting. Advanced Materials, 2020, 32, e1908201.	21.0	84
21	3D core/shell hierarchies of MnOOH ultrathin nanosheets grown on NiO nanosheet arrays for high-performance supercapacitors. Nano Energy, 2014, 4, 56-64.	16.0	83
22	Flexible Colorimetric Detection of Mercuric Ion by Simply Mixing Nanoparticles and Oligopeptides. Small, 2011, 7, 1407-1411.	10.0	82
23	Oneâ€Dimensional Arrangement of Gold Nanoparticles with Tunable Interparticle Distance. Small, 2009, 5, 2819-2822.	10.0	75
24	A Ni2P nanocrystal cocatalyst enhanced TiO2 photoanode towards highly efficient photoelectrochemical water splitting. Chemical Engineering Journal, 2020, 385, 123878.	12.7	71
25	Threeâ€Phase Electrolysis by Gold Nanoparticle on Hydrophobic Interface for Enhanced Electrochemical Nitrogen Reduction Reaction. Advanced Science, 2020, 7, 2002630.	11.2	69
26	Pd Nanoparticle-Decorated 3D-Printed Hierarchically Porous TiO <sub>2</sub> Scaffolds for the Efficient Reduction of a Highly Concentrated 4-Nitrophenol Solution. ACS Applied Materials & Interfaces, 2020, 12, 28100-28109.	8.0	69
27	Ni(OH) <sub>2</sub> /CoO/reduced graphene oxide composites with excellent electrochemical properties. Journal of Materials Chemistry A, 2013, 1, 478-481.	10.3	68
28	<i>In situ</i> decorated Ni <sub>2</sub> P nanocrystal co-catalysts on g-C <sub>3</sub> N <sub>4</sub> for efficient and stable photocatalytic hydrogen evolution <i>via</i> a facile co-heating method. Journal of Materials Chemistry A, 2020, 8, 2995-3004.	10.3	68
29	Proteinâ€Based Memristive Nanodevices. Small, 2011, 7, 3016-3020.	10.0	67
30	Nanoscaled Surface Patterning of Conducting Polymers. Small, 2011, 7, 1309-1321.	10.0	64
31	Tailoring the Salt Transport Flux of Solar Evaporators for a Highly Effective Salt-Resistant Desalination with High Productivity. ACS Nano, 2022, 16, 2511-2520.	14.6	64
32	Patterning of Plasmonic Nanoparticles into Multiplexed One-Dimensional Arrays Based on Spatially Modulated Electrostatic Potential. ACS Nano, 2011, 5, 8288-8294.	14.6	62
33	Visible Photoresponse of Singleâ€Layer Graphene Decorated with TiO <sub>2</sub> Nanoparticles. Small, 2013, 9, 2076-2080.	10.0	58
34	Programmable Negative Differential Resistance Effects Based on Selfâ€Assembled Au@PPy Core–Shell Nanoparticle Arrays. Advanced Materials, 2018, 30, e1802731.	21.0	58
35	A self-supporting bimetallic Au@Pt core-shell nanoparticle electrocatalyst for the synergistic enhancement of methanol oxidation. Scientific Reports, 2017, 7, 6347.	3.3	56
36	Tunable random lasing behavior in plasmonic nanostructures. Nano Convergence, 2017, 4, 1.	12.1	54

#	Article	IF	CITATIONS
37	Beyond Skin Pressure Sensing: 3D Printed Laminated Graphene Pressure Sensing Material Combines Extremely Low Detection Limits with Wide Detection Range. Advanced Functional Materials, 2022, 32, .	14.9	54
38	Colorimetric Chemodosimeter Based on Diazonium–Goldâ€Nanoparticle Complexes for Sulfite Ion Detection in Solution. Small, 2012, 8, 3412-3416.	10.0	53
39	Synergistic Modulation of Surface Interaction to Assemble Metal Nanoparticles into Twoâ€Dimensional Arrays with Tunable Plasmonic Properties. Small, 2014, 10, 609-616.	10.0	51
40	Towards active plasmonic response devices. Nano Research, 2015, 8, 406-417.	10.4	51
41	Highâ€Performance and Stable Organic Transistors and Circuits with Patterned Polypyrrole Electrodes. Advanced Materials, 2012, 24, 2159-2164.	21.0	50
42	Free-standing one-dimensional plasmonic nanostructures. Nanoscale, 2012, 4, 66-75.	5.6	46
43	Neutral Mononuclear Copper(I) Complexes: Synthesis, Crystal Structures, and Photophysical Properties. Inorganic Chemistry, 2016, 55, 5845-5852.	4.0	45
44	Enhanced Photoresponse of Conductive Polymer Nanowires Embedded with Au Nanoparticles. Advanced Materials, 2016, 28, 2978-2982.	21.0	45
45	Synthesis of Fivefold Stellate Polyhedral Gold Nanoparticles with {110}â€Facets via a Seedâ€Mediated Growth Method. Small, 2013, 9, 705-710.	10.0	43
46	Printed Honeycomb-Structured Reduced Graphene Oxide Film for Efficient and Continuous Evaporation-Driven Electricity Generation from Salt Solution. ACS Applied Materials & Interfaces, 2021, 13, 26989-26997.	8.0	42
47	pH-dependent aggregation of citrate-capped Au nanoparticles induced by Cu2+ ions: The competition effect of hydroxyl groups with the carboxyl groups. Colloids and Surfaces A: Physicochemical and Engineering Aspects, 2009, 346, 216-220.	4.7	38
48	Uniform and reproducible plasmon-enhanced fluorescence substrate based on PMMA-coated, large-area Au@Ag nanorod arrays. Nano Research, 2018, 11, 953-965.	10.4	38
49	Tapeâ€Imprinted Hierarchical Lotus Seedpodâ€Like Arrays for Extraordinary Surfaceâ€Enhanced Raman Spectroscopy. Small, 2019, 15, e1804527.	10.0	38
50	pH-Dependent Aggregation of Histidine-Functionalized Au Nanoparticles Induced by Fe <sup>3+</sup> lons. Journal of Physical Chemistry C, 2008, 112, 3267-3271.	3.1	37
51	Enhanced Electrical Conductivity of Individual Conducting Polymer Nanobelts. Small, 2011, 7, 1949-1953.	10.0	37
52	Semiconductive, Oneâ€Dimensional, Selfâ€Assembled Nanostructures Based on Oligopeptides with Ï€â€Conjugated Segments. Chemistry - A European Journal, 2011, 17, 4746-4749.	3.3	35
53	Coral-like PdCu Alloy Nanoparticles Act as Stable Electrocatalysts for Highly Efficient Formic Acid Oxidation. ACS Sustainable Chemistry and Engineering, 2019, 7, 15354-15360.	6.7	34
54	Spatial Distribution Recast for Organic Bulk Heterojunctions for Highâ€Performance Allâ€Inorganic Perovskite/Organic Integrated Solar Cells. Advanced Energy Materials, 2020, 10, 2000851.	19.5	34

#	Article	IF	CITATIONS
55	Woodâ€Inspired Binder Enabled Vertical 3D Printing of g <sub>3</sub> N <sub>4</sub> /CNT Arrays for Highly Efficient Photoelectrochemical Hydrogen Evolution. Advanced Functional Materials, 2021, 31, 2105045.	14.9	34
56	pH-dependent response of citrate capped Au nanoparticle to Pb2+ ion. Colloids and Surfaces A: Physicochemical and Engineering Aspects, 2008, 325, 194-197.	4.7	32
57	Heterostructures of vertical, aligned and dense SnO2 nanorods on graphene sheets: in situ TEM measured mechanical, electrical and field emission properties. Journal of Materials Chemistry, 2012, 22, 19196.	6.7	29
58	Enabling low amounts of YAC:Ce <sup>3+</sup> to convert blue into white light with plasmonic Au nanoparticles. Nanoscale, 2015, 7, 10350-10356.	5.6	28
59	3D-printed endoplasmic reticulum rGO microstructure based self-powered triboelectric pressure sensor. Chemical Engineering Journal, 2022, 445, 136821.	12.7	28
60	Rational Design of Plasmonic Metal Nanostructures for Solar Energy Conversion. CCS Chemistry, 2022, 4, 1153-1168.	7.8	27
61	3D Printing of Powderâ€Based Inks into Functional Hierarchical Porous TiO <sub>2</sub> Materials. Advanced Engineering Materials, 2020, 22, 1901088.	3.5	26
62	Scalable Fabrication of Multiplexed Plasmonic Nanoparticle Structures Based on AFM Lithography. Small, 2016, 12, 5818-5825.	10.0	25
63	A conductive polyacrylamide hydrogel enabled by dispersion-enhanced MXene@chitosan assembly for highly stretchable and sensitive wearable skin. Journal of Materials Chemistry B, 2021, 9, 8862-8870.	5.8	25
64	The Electrode's Effect on the Stability of Organic Transistors and Circuits. Advanced Materials, 2012, 24, 3053-3058.	21.0	24
65	Chemically tunable photoresponse of ultrathin polypyrrole. Nanoscale, 2017, 9, 7760-7764.	5.6	24
66	Multishelled Hollow Structures of Yttrium Oxide for the Highly Selective and Ultrasensitive Detection of Methanol. Small, 2019, 15, e1804688.	10.0	22
67	Coordination competition-driven synthesis of triple-shell hollow α-Fe2O3 microspheres for lithium ion batteries. Electrochimica Acta, 2019, 306, 151-158.	5.2	22
68	150Ânm × 200Ânm Crossâ€Point Hexagonal Boron Nitrideâ€Based Memristors. Advanced Electronic Materials, 2020, 6, 1900115.	5.1	22
69	A method for joining individual graphene sheets. Carbon, 2012, 50, 4965-4972.	10.3	21
70	Lasing behavior of surface functionalized carbon quantum dot/RhB composites. Nanoscale, 2017, 9, 5049-5054.	5.6	21
71	Localized surface plasmon resonance enhanced electrochemical nitrogen reduction reaction. Applied Catalysis B: Environmental, 2022, 301, 120808.	20.2	20
72	Micro Organic Light Emitting Diode Arrays by Patterned Growth on Structured Polypyrrole. Advanced Optical Materials, 2020, 8, 1902105.	7.3	19

#	Article	IF	CITATIONS
73	In-situ phase transition induced nanoheterostructure for overall water splitting. Chemical Engineering Journal, 2021, 409, 128156.	12.7	19
74	Engineering Surface Plasmons in Metal/Nonmetal Structures for Highly Desirable Plasmonic Photodetectors. , 2022, 4, 343-355.		19
75	Buffer-Layer-Assisted Epitaxial Growth of Perfectly Aligned Oxide Nanorod Arrays in Solution. Crystal Growth and Design, 2011, 11, 4885-4891.	3.0	17
76	Morphological effects on the selectivity of intramolecular versus intermolecular catalytic reaction on Au nanoparticles. Nanoscale, 2017, 9, 7727-7733.	5.6	17
77	Ultrahigh Field Enhancement Optimization Versus Rabi Splitting Investigated Using Au Nano-Bipyramids on Metal Films. Journal of Physical Chemistry C, 2019, 123, 12984-12996.	3.1	17
78	Vertical 3D Printed Forestâ€Inspired Hierarchical Plasmonic Superstructure for Photocatalysis. Advanced Functional Materials, 2021, 31, 2100768.	14.9	17
79	In Situ Growth of Co <sub>2</sub> P Nanocrystal on g-C <sub>3</sub> N <sub>4</sub> for Efficient and Stable Photocatalytic Hydrogen Evolution. Energy & Fuels, 2021, 35, 1859-1865.	5.1	16
80	A large scaled-up monocrystalline 3R MoS <sub>2</sub> electrocatalyst for efficient nitrogen reduction reactions. New Journal of Chemistry, 2021, 45, 2488-2495.	2.8	15
81	Highly Sensitive Electroâ€Plasmonic Switches Based on Fivefold Stellate Polyhedral Gold Nanoparticles. Small, 2015, 11, 5395-5401.	10.0	14
82	Resonant modes of reflecting gratings engineered for multimodal sensing. APL Photonics, 2020, 5, 076108.	5.7	14
83	Multiplexed Assembly of Plasmonic Nanostructures Through Charge Inversion on Substrate for Surface Encoding. ACS Applied Materials & amp; Interfaces, 2020, 12, 6176-6182.	8.0	14
84	Oxygenâ€Tolerant RAFT Polymerization Catalyzed by a Recyclable Biomimetic Mineralization Enhanced Biological Cascade System. Macromolecular Rapid Communications, 2022, 43, e2100559.	3.9	13
85	Spectral plasmonic effect in the nano-cavity of dye-doped nanosphere-based photonic crystals. Nanotechnology, 2016, 27, 165703.	2.6	12
86	Modulating the Spatial Electrostatic Potential for 1D Colloidal Nanoparticles Assembly. Advanced Materials Interfaces, 2017, 4, 1700505.	3.7	12
87	Nanostructured hexagonal ReO <sub>3</sub> with oxygen vacancies for efficient electrocatalytic hydrogen generation. Nanotechnology, 2019, 30, 355701.	2.6	12
88	Lithographical Fabrication of Organic Single-Crystal Arrays by Area-Selective Growth and Solvent Vapor Annealing. ACS Applied Materials & Interfaces, 2020, 12, 48854-48860.	8.0	12
89	Plasmonic Nanoparticle Film for Low-Power NIR-Enhanced Photocatalytic Reaction. ACS Applied Materials & amp; Interfaces, 2020, 12, 16753-16761.	8.0	12
90	Preparation of titanium dioxide and barium titanate nanothick film by Langmuir–Blodgett technique. Thin Solid Films, 2000, 379, 218-223.	1.8	11

#	Article	IF	CITATIONS
91	One-step integration of a multiple-morphology gold nanoparticle array on a TiO <sub>2</sub> film <i>via</i> a facile sonochemical method for highly efficient organic photovoltaics. Journal of Materials Chemistry A, 2018, 6, 8419-8429.	10.3	11
92	Interface Engineering of Colloidal CdSe Quantum Dot Thin Films as Acid-Stable Photocathodes for Solar-Driven Hydrogen Evolution. ACS Applied Materials & Interfaces, 2018, 10, 17129-17139.	8.0	11
93	Plasmonic Metal Nanostructures as Efficient Light Absorbers for Solar Water Splitting. Advanced Energy and Sustainability Research, 2021, 2, 2100092.	5.8	11
94	Chemical Reaction on a Solid Surface with Nanoconfined Geometry. Small, 2012, 8, 333-335.	10.0	10
95	Plasmonic nanoparticle-film-assisted photoelectrochemical catalysis across the entire visible-NIR region. Nanoscale, 2019, 11, 23058-23064.	5.6	10
96	Fabrication of tunable aluminum nanodisk arrays <i>via</i> a self-assembly nanoparticle template method and their applications for performance enhancement in organic photovoltaics. Journal of Materials Chemistry A, 2018, 6, 3649-3658.	10.3	9
97	Positioning growth of NPB crystalline nanowires on the PTCDA nanocrystal template. Nanoscale, 2018, 10, 10262-10267.	5.6	9
98	PdAg Nanoparticles with Different Sizes: Facile Oneâ€Step Synthesis and High Electrocatalytic Activity for Formic Acid Oxidation. Chemistry - an Asian Journal, 2021, 16, 34-38.	3.3	9
99	The coordination sites of phosphorothioate OligoG10 with Cd2+ and CdS nanoparticles. New Journal of Chemistry, 2003, 27, 823-826.	2.8	8
100	Highâ€Yield Synthesis of Au@Ag Right Bipyramids and Selfâ€Assembly into Fourâ€Leafâ€Cloverâ€like Structures. Particle and Particle Systems Characterization, 2018, 35, 1700114.	2.3	8
101	Assembly of Au Nanoparticles with Anisotropic Optical Property Directed by 2′-Phosphorothioate Oligo-DNA. Chinese Journal of Chemistry, 2005, 23, 1143-1145.	4.9	5
102	Self-generating nanogaps for highly effective surface-enhanced Raman spectroscopy. Nano Research, 2022, 15, 3496-3503.	10.4	5
103	A facile method for fabrication of highly integrated organic field-effect transistors on photoresist-unwettable insulators with remarkable stability. Organic Electronics, 2016, 34, 104-110.	2.6	4
104	Growing Inâ€Plane Multiplex Plasmonic Arrays for Synergistic Enhanced Photocurrent Response. Advanced Materials Interfaces, 2020, 7, 1900966.	3.7	4
105	Facile fabrication of a single-particle platform with high throughput via substrate surface potential regulated large-spacing nanoparticle assembly. Nano Research, 0, , 1.	10.4	4
106	Facile and Surfactantâ€Free Routed Spherical Au@Pt Core–Shell–Satellite Nanoparticles as Highâ€Efficient and Stable Electrocatalyst for Methanol Oxidation. Energy Technology, 2022, 10, .	3.8	4
107	Conductance measurements of individual polypyrrole nanobelts. Nanoscale, 2015, 7, 2301-2305.	5.6	3
108	Stamp recyclable contact printing of liquid droplet matrix on various surfaces. Journal of Materials Chemistry C, 2017, 5, 10971-10975.	5.5	3

#	Article	IF	CITATIONS
109	Double-sided asymmetric surface modification of ZnO interfacial layer to enhance performance in organic solar cells. Applied Physics Letters, 2019, 115, .	3.3	3
110	Strategies for High Resolution Patterning of Conducting Polymers. , 0, , .		2
111	Quasi-3-D Au mushrooms with programmable morphology for high-capacity flexible plasmonic encoding. Science China Materials, 2022, 65, 2227-2234.	6.3	2
112	Cadmium ion induced bending of phosphorothioate oligonucleotide G10. Physical Chemistry Chemical Physics, 2003, 5, 632-634.	2.8	1
113	Enabling low amounts of YAG:Ce3+ to convert blue into white light with plasmonic Au nanoparticlesâ $\in$ . , 2015, , .		1
114	DNA-Templated Formation of Needle-like CdS Nanoparticles in Langmuir-Blodgett Film. Molecular Crystals and Liquid Crystals, 2001, 371, 49-52.	0.3	0
115	Conversion Between Two-Dimensional Square and Hexagonal Close-Packed Architectures in Aggregates of Au Nanoparticles Mediated by Bending DNA Linkers. Journal of Nanoscience and Nanotechnology, 2009, 9, 2055-2060.	0.9	0